Paper 223

Proceedings of the Seventh International Conference on Computational Structures Technology, B.H.V. Topping and C.A. Mota Soares (Editors), Civil-Comp Press, Stirling, Scotland.

Wheel-Rail Contact Forces in High-Speed Simply Supported Bridges at Resonance

P. Museros†, A. Castillo-Linares† and E. Alarcón‡
†Department of Structural Mechanics
Superior School of Civil Engineering, University of Granada, Spain
‡Department of Structural Mechanics and Industrial Constructions
Superior School of Industrial Engineering, Technical University of Madrid, Spain

Abstract

This paper investigates the evolution of the wheel–rail contact forces in high-speed railway bridges during resonance situations. Based on a dimensionless formulation of the equations of motion, a parametric study is conducted and the fundamental parameters influencing the contact forces are brought to light. The bridge is idealised as an Euler–Bernoulli beam, while the train is simulated by a system of rigid bodies, springs and dampers. The situations such that a severe reduction of the contact force could take place are identified and compared with actual bridges. Finally, a real case is analysed and checked against the theoretical model.

Keywords: wheel–rail contact forces, derailment, train–bridge interaction, moving loads, dynamics of bridges, high-speed bridges, flexural vibrations.

1 Introduction

The dynamic analysis of high-speed bridges is an active field of research at the moment, as the large number of recent related papers published in specialized journals, conferences and technical workshops demonstrates.

High-speed trains can induce severe vibrations in railway bridges, especially in simply supported ones. Moreover, the operating speeds of modern trains are elevated enough to create resonance situations, which represent some of the most demanding scenarios from the point of view of structural design. Therefore, it is of great interest to produce mathematical models capable of reproducing accurately the behaviour of bridges at resonance with a low computational cost. The present paper deals with some of the aspects related to these models, particularly the analysis of wheel–rail contact forces.

The D–214 Committee of the *European Rail Research Institute* (ERRI D–214), as well as the authors, have investigated the train–bridge interaction effects and have found that such phenomenon reduces the structural response in resonance conditions (see [2], [3], [8], [9] and [10]). The following two examples show how these effects are beneficial and can have an influence on the verification of the Serviceability Limits (SLI) of the bridges.

The first example (Figure 1) shows the maximum vertical acceleration at mid–span for a 25 m, simply supported, prestressed concrete box girder bridge carrying two tracks. The mass per unit length of the bridge is 22000 kg/m, the fundamental frequency is 6 Hz, and 1% structural damping has been considered. Only the contribution of the first bending mode has been taken into account. The bridge has been analysed under the passage of an Eurostar train that induces a resonance at 417 km/h. Modern European regulations prescribe a maximum speed for the analysis of 420 km/h (350 km/h multiplied by a security factor 1.2), and a maximum permissible acceleration of the deck equal to 3.5 m/s^2 for ballasted tracks. As can be seen from Figure 1, the maximum acceleration of the bridge at mid–span exceeds this limitation (horizontal dashed line). In such a situation the bridge should be redesigned in order to satisfy this particular SLI.

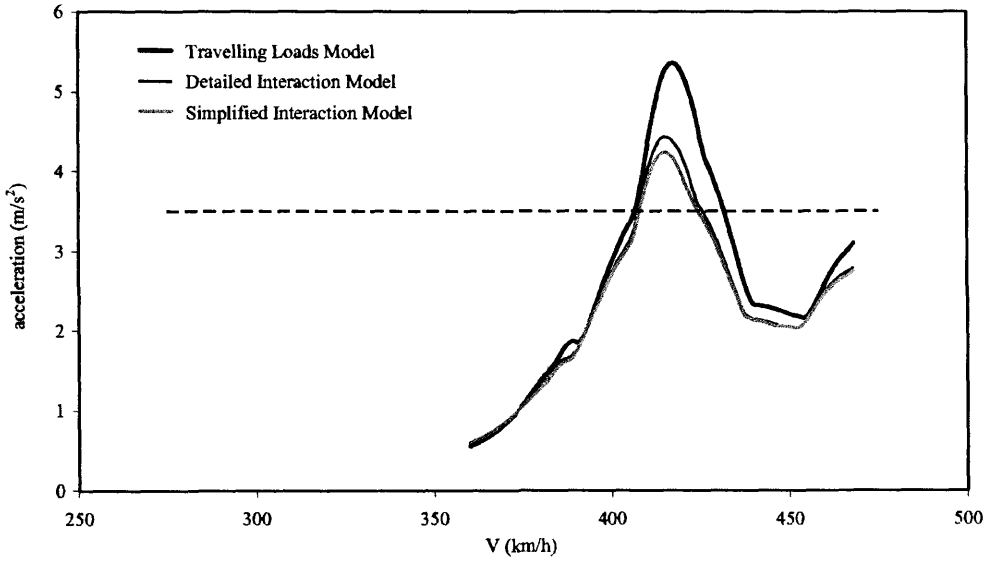

Figure 1. Maximum acceleration at mid–span for a 25 m simply supported PC bridge under the passage of a Eurostar train.

In Figure 1 three different curves are shown. The first one is a plot of the acceleration obtained with a Moving Loads or Travelling Loads Model (TLM). In such model the train axles are considered to transmit concentrated, constant–valued loads, and therefore the train–bridge interaction is disregarded (*i.e.* the inertia of the moving vehicle, as well as the effects of its suspension devices, are not accounted for). As the authors showed in [**9**], the TLM can be too pessimistic in certain situations, especially when the response at resonance is being computed and the frequencies of the primary suspension and fundamental mode of the bridge are similar. Since the frequency of the Eurostar primary suspension is close to 6 Hz, this is precisely the situation corresponding to Figure 1.

In such case, carrying out an analysis with *Interaction Models* can be more convenient. Two of these models are the Detailed Interaction Model (DIM) and the Simplified Interaction Model (SIM). Both are fully described at the end of this Section. As can be seen in Figure 1, the response predicted by both models is very similar, which favours the use of the latter due to its lower computational cost. For the 25 m bridge considered, the maximum acceleration surpasses the limit regardless of the model of the train used in the analysis; nevertheless, the difficulties encountered during the redesign of the bridge would be directly related to the percentage by which the limit is exceed, and therefore the Interaction Models could simplify the task considerably.

The second example (Figure 2) shows the maximum acceleration at mid–span for an 18.7 m, simply supported, prestressed concrete box girder bridge carrying one track. In this case the mass per unit length is 11500 kg/m and the fundamental frequency is 7 Hz. Again, 1% structural damping has been considered and the fundamental bending mode is the only one included in the bridge model.

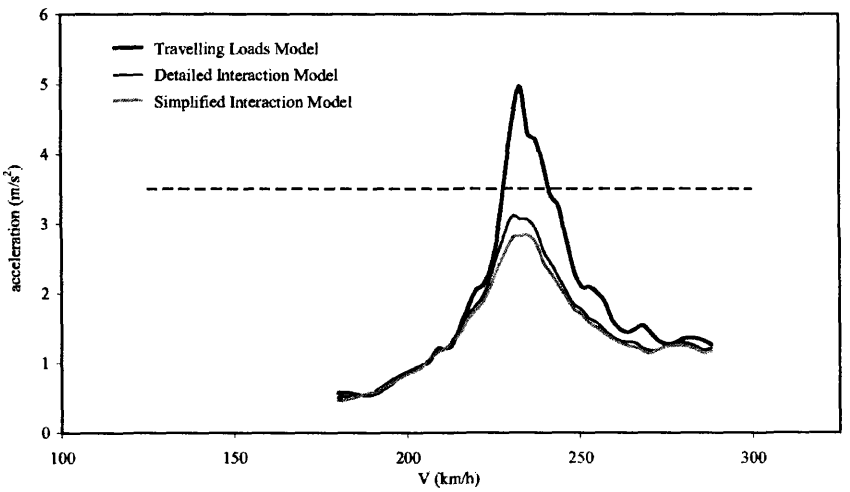

Figure 2. Maximum acceleration at mid–span for a 18.7 m simply supported PC bridge under the passage of a Eurostar train.

As can be seen from that figure, the interaction effects are again beneficial and the bridge even satisfies the acceleration SLI if these are taken into account in the model.

The Eurostar train used in the previous examples has two identical, conventional power cars, one at each extreme of the train. The centre of gravity of the power cars is located midway from each of their two bogies. The characteristics of the power cars, as well as those of the rest of the elements of the train, are summarized in Figure 3 and Table 1. Besides, the Eurostar train considered in the present study contains two identical ensembles of nine passenger cars. Each ensemble is not symmetrical, *i.e.* the intermediate cars (from the second to the eighth) are identical, but the first and ninth cars are different from each other, as well as different from the intermediate ones. Also, the two ensembles are located consecutively, but in such a way that the whole train isn't symmetrical either (the first car of the first ensemble is equal to the first car of the second ensemble, the intermediate cars are identical in both ensembles, and again the ninth cars of both ensembles are equal to each other). In Figure 3 only two intermediate cars are represented but, as stated previously, seven exist in reality. First car is on the left. End car is on the right. Numerical values for all parameters are given in Table 1.

The Detailed Interaction Model of the Eurostar is presented in Figure 3. The ensembles of passenger cars consist of articulated car–bodies resting on a secondary suspension system; the secondary suspension links the joints between two adjacent cars with a single shared bogie, which is itself conventional and carries two wheelsets connected to the bogie by two identical primary suspensions. It is assumed that the power cars do not interact with the passenger cars as regards the vertical and pitching motions. Besides, all car–bodies, bogies and wheelsets are treated as rigid bodies.

Conversely, the Simplified Interaction Model neglects the inertia of the car–bodies and the effects of the secondary suspension. In principle this is acceptable because the natural frequencies associated to the motion of the car–bodies are very low and this fact should prevent their interaction with the bridge (see [**9**]). Also, the SIM represents the motion of the bogies in a simplified way by assuming that half the mass of the bogie vibrates in a purely vertical motion on top of each wheelset. Therefore, the SIM consists of a series of single–degree–of–freedom (SDOF) systems attached to their corresponding wheelset and subjected to a static load that represents the weight of the car–bodies (see Figure 4). In short, the SIM of any train can derived from the DIM by dividing the mass of each bogie into two translational masses, placing each of them on top of the corresponding wheelset; the primary suspensions remain unmodified; the secondary suspensions and the car–bodies are eliminated, and the corresponding part of their static weight is transferred to each half–bogie.

As regards the bridge, the most usual model is the Euler–Bernoulli 2D beam. Finite Element discretizations or modal superposition based on analytic mode shapes are the preferred procedures for simulating its behaviour.

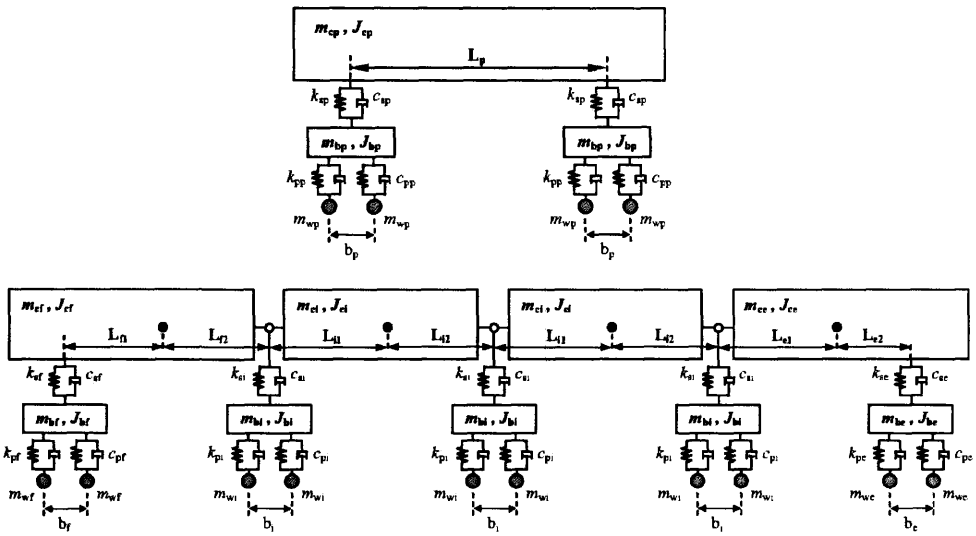

Figure 3. Mechanical model of one power car and one ensemble of passenger cars of a Eurostar train (Detailed Interaction Model)

In the technical literature it is commonly accepted that the wheels remain in contact with the rails at all times (see [1], [5], [7], [12], [13]). Since the vibration of the track and the ballast is ignored in the model, this hypothesis is equivalent to accepting that the wheels never lose contact with the bridge. If the interaction or contact forces between train and bridge are considered positive when their action on the wheels is directed upwards (*i.e.* positive in *normal* conditions), the assumption of a permanent contact between train and wheel implies that these contact forces remain always positive.

The purpose of the present paper is to further investigate if this condition is satisfied during resonance situations and, simultaneously, to bring to light the most important factors that influence the variation of the wheel–rail contact forces.

Power cars	Distance between centres of gravity of the bogies (L_p)	14 m
	Length of the bogie (b_p)	3 m
	Mass of the car–body (m_{cp})	51500 kg
	Centroidal moment of inertia of the car–body (J_{cp})	$1.05 \cdot 10^6$ kg·m^2
	Mass of the bogie (m_{bp})	2200 kg
	Centroidal moment of inertia of the bogie (J_{bp})	1900 kg·m^2
	Mass of the wheelset (m_{wp})	1700 kg
	Stiffness of the primary suspension (k_{pp})	$2.6 \cdot 10^6$ N/m
	Damping coefficient of the primary suspension (c_{pp})	$1.2 \cdot 10^4$ N·s/m
	Stiffness of the secondary suspension (k_{sp})	$3.26 \cdot 10^6$ N/m
	Damping coefficient of the secondary suspension (c_{sp})	$9 \cdot 10^4$ N·s/m
First passenger car	Distance between centres of gravity of car–body and front bogie (L_{f1})	5.448 m
	Distance between centres of gravity of car–body and rear bogie (L_{f2})	13.252 m
	Length of the bogie (b_f)	3 m
	Mass of the car–body (m_{cf})	35860 kg
	Centroidal moment of inertia of the car–body (J_{cf})	$1.658 \cdot 10^6$ kg·m^2
	Mass of the bogie (m_{bf})	2200 kg
	Centroidal moment of inertia of the bogie (J_{bf})	1900 kg·m^2
	Mass of the wheelset (m_{wf})	1700 kg
	Stiffness of the primary suspension (k_{pf})	$2.6 \cdot 10^6$ N/m
	Damping coefficient of the primary suspension (c_{pf})	$1.2 \cdot 10^4$ N·s/m
	Stiffness of the secondary suspension (k_{sf})	$0.9 \cdot 10^5$ N/m
	Damping coefficient of the secondary suspension (c_{sf})	$2 \cdot 10^4$ N·s/m
Intermed. passenger cars	Distance between centres of gravity of car–body and front bogie (L_{i1})	8.926 m
	Distance between centres of gravity of car–body and rear bogie (L_{i2})	**9.774 m**
	Length of the bogie (b_i)	**3 m**
	Mass of the car–body (m_{ci})	**22525 kg**
	Centroidal moment of inertia of the car–body (J_{ci})	**$8.1 \cdot 10^5$ kg·m^2**
	Mass of the bogie (m_{bi})	**2900 kg**
	Centroidal moment of inertia of the bogie (J_{bi})	**2508 kg·m^2**
	Mass of the wheelset (m_{wi})	**1900 kg**
	Stiffness of the primary suspension (k_{pi})	**$2 \cdot 10^6$ N/m**
	Damping coefficient of the primary suspension (c_{pi})	**$1.2 \cdot 10^4$ N·s/m**
	Stiffness of the secondary suspension (k_{si})	**$0.58 \cdot 10^6$ N/m**
	Damping coefficient of the secondary suspension (c_{si})	**$2 \cdot 10^4$ N·s/m**
Last (end) passenger car	Distance between centres of gravity of car–body and front bogie (L_{e1})	**10.99 m**
	Distance between centres of gravity of car–body and rear bogie (L_{e2})	**7.71 m**
	Length of the bogie (b_e)	**3 m**
	Mass of the car–body (m_{ce})	**27122 kg**
	Centroidal moment of inertia of the car–body (J_{ce})	**$1.254 \cdot 10^6$ kg·m^2**
	Mass of the bogie (m_{be})	**2900 kg**
	Centroidal moment of inertia of the bogie (J_{be})	**2508 kg·m^2**
	Mass of the wheelset (m_{we})	**1900 kg**
	Stiffness of the primary suspension (k_{pe})	**$1.32 \cdot 10^6$ N/m**
	Damping coefficient of the primary suspension (c_{pe})	**$1.2 \cdot 10^4$ N·s/m**
	Stiffness of the secondary suspension (k_{se})	**$0.25 \cdot 10^6$ N/m**
	Damping coefficient of the secondary suspension (c_{se})	**$2 \cdot 10^4$ N·s/m**

Table 1. Mechanical characteristics of the Eurostar train as required for the Detailed Interaction Model

Auxiliary distances	Distance between consecutive wheels of a power car and a passenger car	**3.275 m**
	Distance between the last wheel of the first ensemble of passenger cars and the first wheel of the second ensemble	**3.52 m**
	Total length of the train	**386.67 m**

Table 1 (continued). Mechanical characteristics of the Eurostar train as required for the Detailed Interaction Model

2 Mathematical Model

2.1 Generic Equations of an Interaction Model

Many authors have presented equations of motion for train–bridge models, some of them based on a Finite Element Method discretization of the bridge (see [**5**], [**12**], [**13**]), others based on analytic mode shapes (see [**6**], [**9**]).

In this section a compact form of these equations is presented that allows a general expression of the interaction forces to be derived. No complete mathematical justification will be given, since this can be easily accomplished from the results presented in any of the aforementioned references. The equations of motion of a train–bridge system can be written in the following manner:

$$\begin{bmatrix} M_b + A^T M_{ww} A & 0 \\ 0 & M_{tt} \end{bmatrix} \begin{bmatrix} \ddot{\underline{\xi}} \\ \ddot{\underline{z}}_t \end{bmatrix} + \begin{bmatrix} C_b + A^T C_{ww} A & A^T C_{wt} \\ C_{tw} A & C_{tt} \end{bmatrix} \begin{bmatrix} \dot{\underline{\xi}} \\ \dot{\underline{z}}_t \end{bmatrix} + \\ + \begin{bmatrix} K_b + A^T K_{ww} A & A^T K_{wt} \\ K_{tw} A & K_{tt} \end{bmatrix} \begin{bmatrix} \underline{\xi} \\ \underline{z}_t \end{bmatrix} = \begin{bmatrix} A^T \left(\underline{F}_{gw} - K_{wt} K_{tt}^{-1} \underline{F}_{gt} \right) \\ \underline{0} \end{bmatrix} \tag{1}$$

In Equation (1) M_b, C_b and K_b represent the mass, damping and stiffness matrices of the bridge. Vector $\underline{\xi}(t)$ contains the degrees of freedom of the bridge model, *i.e.* either the Finite Element degrees of freedom *or* the modal amplitudes, depending on the approach adopted for simulating the behaviour of the Euler–Bernoulli beam. Vector $\underline{z}_t(t)$ contains the degrees of freedom of the train: vertical motion and pitching rotation of car–bodies and bogies if the DIM is used; vertical motion of the half–bogies for the SIM. Vector $\underline{F}_{gt}$ is the gravity load vector associated to the degrees of freedom in $\underline{z}_t(t)$; the static loads acting on the half–bogies must be included if the SIM is being used. $\underline{F}_{gw}$ is a gravity load vector containing the static weights of the wheelsets in order (the first element in $\underline{F}_{gw}$ is the weight of the first wheelset, the second element is the weight of the second wheelset, and so on). The motions of bridge and train are computed from their static equilibrium positions.

Also in Equation (1), matrices M_{tt}, M_{ww}, C_{tt}, C_{tw}, C_{wt}, C_{ww}, K_{tt}, K_{tw}, K_{wt}, K_{ww}, are submatrices corresponding to the dynamic equation of motion of the train when isolated from the bridge. If the degrees of freedom of the train $\underline{z}_t(t)$ and the vertical motions of the wheelsets $\underline{z}_w(t)$ are combined into a single vector, the matrix equation of motion of the train separated from the bridge is:

$$\begin{bmatrix} M_{tt} & 0 \\ 0 & M_{ww} \end{bmatrix} \begin{bmatrix} \ddot{\underline{z}}_t \\ \ddot{\underline{z}}_w \end{bmatrix} + \begin{bmatrix} C_{tt} & C_{tw} \\ C_{wt} & C_{ww} \end{bmatrix} \begin{bmatrix} \dot{\underline{z}}_t \\ \dot{\underline{z}}_w \end{bmatrix} + \begin{bmatrix} K_{tt} & K_{tw} \\ K_{wt} & K_{ww} \end{bmatrix} \begin{bmatrix} \underline{z}_t \\ \underline{z}_w \end{bmatrix} = \begin{bmatrix} \underline{0} \\ \underline{F}_{gw} - K_{wt} K_{tt}^{-1} \underline{F}_{gt} + \underline{F}(t) \end{bmatrix} \tag{2}$$

where $\underline{F}(t)$ is the vector containing the interaction of contact forces acting on the wheels. As stated, before forces are considered positive if directed upwards. These forces are the ones that move the bridge from its static equilibrium position; the motion of the bridge is governed by the following equation:

$$M_b \ddot{\underline{\xi}} + C_b \dot{\underline{\xi}} + K_b \underline{\xi} = -A^T \underline{F}(t) \tag{3}$$

Finally, matrix A in Equation (1) relates the vertical motion of the wheels to the degrees of freedom of the bridge. The same matrix in Equation (3) transforms the concentrated loads $\underline{F}(t)$ into the load vector of the bridge. The precise form of matrix A depends therefore on the model adopted for the bridge. Since the wheels are assumed to be in contact with the bridge at all times, their vertical position at a given time is equal to the vertical displacement of the corresponding section of the bridge. This relation is expressed simply as:

$$\underline{z}_w(t) = A \cdot \underline{\xi}(t) \tag{4}$$

Matrix A depends on the position of the wheels along the bridge, and therefore is time-dependent. Equation (1), consequently, is a second-order differential equation with variable coefficients. The effect of the centrifugal and Coriolis accelerations is not considered in Equation (1) because, according to Yang et al. [**14**], the deflections of high-speed bridges are small enough to neglect its influence. As a result, the vertical velocities and accelerations of the wheels can be computed as:

$$\dot{\underline{z}}_w(t) = A \cdot \dot{\underline{\xi}}(t) \qquad \ddot{\underline{z}}_w(t) = A \cdot \ddot{\underline{\xi}}(t) \tag{5}$$

Finally, the interaction forces are obtained from Equations (2), (4) and (5) in the following form:

$$\underline{F}(t) = -\underline{F}_{gw} + M_{ww} A \ddot{\underline{\xi}} + C_{wt} \dot{\underline{z}}_t + C_{ww} A \dot{\underline{\xi}} + K_{wt} \left(\underline{z}_t + K_{tt}^{-1} \underline{F}_{gt} \right) + K_{ww} A \underline{\xi} \tag{6}$$

2.2 Wheel–Rail Contact Forces in the Simplified Interaction Model

If the behaviour of a simply supported Euler–Bernoulli beam is modelled by modal superposition, the modal shapes are the usual family of sines: $sin(i\pi x/L)$, where x is the abscissa along the bridge span L. If the first M modes are considered and the number of axles of the train is N, the interpolation matrix A has dimensions N×M and its elements are as follows:

$$A_{ki}(t)=\begin{cases}\sin\dfrac{i\pi(Vt-d_k)}{L} & 0\le Vt-d_k\le L\\ 0 & \text{otherwise}\end{cases} \tag{6}$$

In Equation (6) V stands for the speed of the train and d_k is the initial distance from the kth load to the beginning of the bridge. In the rest of the paper only the fundamental mode will be taken into account because the interest will be focussed in the resonant response of such mode. The amplitude of the fundamental mode will be represented by $\xi(t)$. Accordingly, the interpolation matrix A transforms into the following vector:

$$A(t)=\begin{bmatrix}\sin\dfrac{\pi(Vt-d_1)}{L}\\ \sin\dfrac{\pi(Vt-d_2)}{L}\\ \vdots\\ \sin\dfrac{\pi(Vt-d_N)}{L}\end{bmatrix} \tag{7}$$

The Simplified Interaction Model is shown in Figure 4. The corresponding matrices in Equation (2) are diagonal and the expression of the contact forces reduces to

$$\underline{F}(t)=-\underline{F}_{gw}-\underline{F}_{gt}+M_{ww}A\ddot{\xi}+C_{wt}\dot{\underline{z}}_t+C_{ww}A\dot{\xi}+K_{wt}\underline{z}_t+K_{ww}A\xi \tag{8}$$

Thus, the expression of the contact force in the kth axle is:

$$\begin{aligned}F_k(t)=m_{wk}g+m_{tk}g+Q_k+m_{wk}\cdot\sin\left(\frac{\pi(Vt-d_k)}{L}\right)\ddot{\xi}+c_{pk}\cdot\sin\left(\frac{\pi(Vt-d_k)}{L}\right)\dot{\xi}+\\ -c_{pk}\dot{z}_{tk}+k_{pk}\cdot\sin\left(\frac{\pi(Vt-d_k)}{L}\right)\xi-k_{pk}z_{tk}\end{aligned} \tag{9}$$

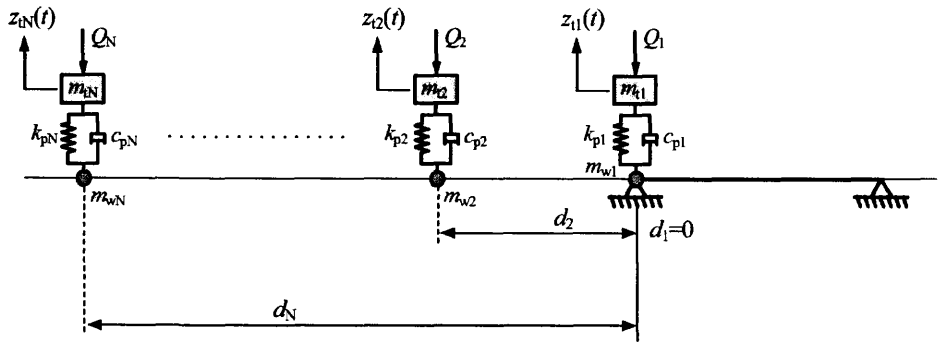

Figure 4. The Simplified Interaction Model.

3 Parametric Study of the Wheel–Rail Contact Forces

3.1 Fundamental Parameters and Ranges of Variation

In a previous contribution to the CST 2002 conference [**9**], the authors presented a formulation of the equations of motion of the SIM based on dimensionless parameters, very similar to one presented by Klasztorny and Langer in [**6**]. In order to analyse the fundamental characteristics of the resonant behaviour of simply supported bridges, a parametric study was conducted in [**9**] using a theoretical train of 15 equally spaced axles. That study will be extended herein with the purpose of investigating the evolution of the wheel–rail contact forces at resonance.

The SIM was adopted as the train model in the aforementioned study, and the mechanical properties of the primary suspensions (k_{pk}, c_{pk}), unsprung masses (m_{wk}), semi–sprung masses (m_{tk}) and static loads (Q_k) were identical for all the axles. The distance between any two consecutive axles was denoted as d. In what follows, the characteristics of the axles will be represented by the symbols k_p, c_p, m_w, m_t and Q.

In such conditions it can easily be established that the contact forces divided by its static value depend only on the values of a number of dimensionless variables called *fundamental parameters*. These parameters are the following: the *frequency ratio* (η), which is the ratio of the frequency of the primary suspension and the frequency of the fundamental mode of the bridge $\eta = n_t/n_0$, where $n_t = (k_p/m_t)^{0.5}/(2\pi)$; the *mass ratio* ($\mu$), quotient of the semi–sprung mass m_t and the total mass of the bridge; the *vehicle mass ratio* $\mu_1 = m_w/m_t$; the ratio between the span of the bridge and the characteristic distance between axles (L/d); the dimensionless speed $\alpha = VT/L$, where $T = 1/n_0$ is the fundamental period; and finally, the damping ratios of the bridge (ζ) and primary suspension

($\zeta_t = c_p/(4\cdot\pi\cdot m_t\cdot n_t)$). Fixed values of 1% and 15% are assigned to these damping ratios, respectively, because they are representative of a large number of real cases. Also, a value $\mu_1 = 4/3$ is taken for the vehicle mass ratio because it is a good approximation to the usual ones in modern trains.

The *normalized contact force* can be derived from the Equation (9) following the dimensionless formulation presented in [**9**]:

$$f_k(\tau) = \frac{F_k(\tau)}{P} = 1 + \frac{1}{4\pi^2}\mu_1\mu\frac{\omega_0^2\cdot mL}{P}\cdot\sin(\alpha\pi(\tau-\tau_k))\xi'' + \\ + \frac{1}{\pi}\zeta_t\eta\mu\frac{\omega_0^2\cdot mL}{P}\cdot(\sin(\alpha\pi(\tau-\tau_k))\xi' - z_k') + \\ + \eta^2\mu\frac{\omega_0^2\cdot mL}{P}\cdot(\sin(\alpha\pi(\tau-\tau_k))\xi - z_k) \qquad (10)$$

where τ is the dimensionless time ($\tau = t/T$), P is the static value of the contact force ($P = m_w g + m_t g + Q$), ω_0 is the fundamental frequency of the bridge in rad/s, m is the mass of the bridge per unit length, τ_k is the instant when the kth load enters the bridge measured in dimensionless time ($\tau_k = (k-1)d/(VT)$), and the dashes denote derivation with respect to dimensionless time.

From the Generalized Similarity Formulas presented in [**9**] it can be deduced that the normalized contact force obtained in Equation (10) is identical in all train–bridge systems having the same values of the fundamental parameters η, μ, μ_1, L/d, α, ζ and ζ_t. The resonance condition implies that $\alpha = d/L$ and, since the values of μ_1, ζ and ζ_t have been fixed, only three independent parameters remain: η, μ and L/d. Realistic ranges of variation of these parameters were also derived in [**9**]:

$$L/d = \{0.3,\ 0.5,\ 0.75,\ 1.0,\ 2.0,\ 4.0\}$$

$$\eta = \{0.3,\ 0.5,\ 0.75,\ 1.0,\ 1.25,\ 1.5,\ 1.75,\ 2.0,\ 3.0,\ 4.0,\ 6.0\}$$

$$0.001 \le \mu \le 0.04$$

Ten discrete values of μ were selected in order to cover the above defined range, in such a way that the quotient between two consecutive values is a constant (see Figures 6, 7 and 8). As regards the intermediate values L/d = 1.5, 2.5, etc., these have been excluded from the analysis since they cause a cancellation of the resonance situation [**14**].

The purpose of Section 3 is to present the results of a parametric analysis of the normalized contact force obtained in Equation (10) in resonance condition, when the fundamental parameters η, μ and L/d vary within the realistic ranges defined previously.

3.2 Results of the Parametric Study

In resonance situation it can be observed that the oscillations of the contact forces of the rear wheels around its static value are more severe than the corresponding to the front ones. This behaviour is in fact what one would expect because, as it is apparent, the vibration of the bridge becomes more and more intense with the passage of the consecutive axles. Figure 5 shows this kind of behaviour for the first example presented in Section 1 (25 m bridge traversed by the Eurostar–DIM travelling at 415 km/h).

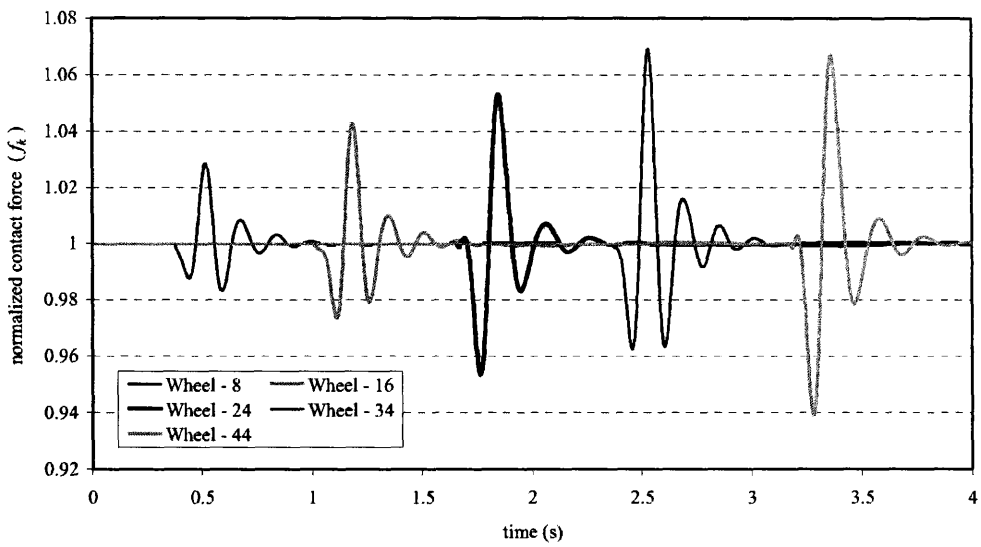

Figure 5. Normalized contact forces in several wheelsets during resonance

In view of this fact, during the completion of the parametric study explained in Section 3.1 it was decided to analyse the contact force corresponding to the 15th axle of the theoretical train of equidistant loads. Thus, the results presented in the rest of this section are referred to this particular axle.

The authors showed in [**11**] that, if the most usual ranges of values of d and T are considered, the first resonance condition ($VT = d$) is not attainable at speed lower than 420 km/h for train–bridge systems having $L/d = 0.3$ or $L/d = 0.5$. Therefore attention will be focussed on the results corresponding to $L/d = 0.75$ and greater.

Figures 6, 7 and 8 show the minimum value of the normalized train interaction force for the 15th axle at resonance when $L/d = 0.75$, $L/d = 1$ and $L/d = 2$, respectively. The results are presented as a function of η and for different values of μ. The vertical thick lines indicate the usual limits of the frequency ratio for each

particular value of L/d. As can be seen, certain combinations of η and μ produce negative values of the minimum contact force for L/d = 0.75 and L/d = 1, which implies that the wheel–rail contact would be lost. These pairs of values (η, μ) have been depicted as diamonds and triangles in Figure 9. The meaning of this figure will be explained in detail at the end of the present section.

On the contrary, for L/d = 2 no situation of loss of contact occurs. Indeed the results of the study have shown that, the greater the L/d ratio, the smaller the probability of a loss of wheel–rail contact. Or, in other words, for increasing values of the L/d ratio the oscillations of the contact forces around its static value are less significant.

Even if these results seem to predict the possibility of loss of contact during resonance for realistic values of η and μ , it must be emphasised that these two fundamental parameters and the L/d ratio are not completely independent of each other. Since the limit values of d are defined by the geometry of actual trains, the L/d ratio tends to increase with the length of the bridge; the longer bridges usually have higher linear masses and lower natural frequencies, and therefore high values of L/d are expected to occur simultaneously with low mass ratios and high frequency ratios.

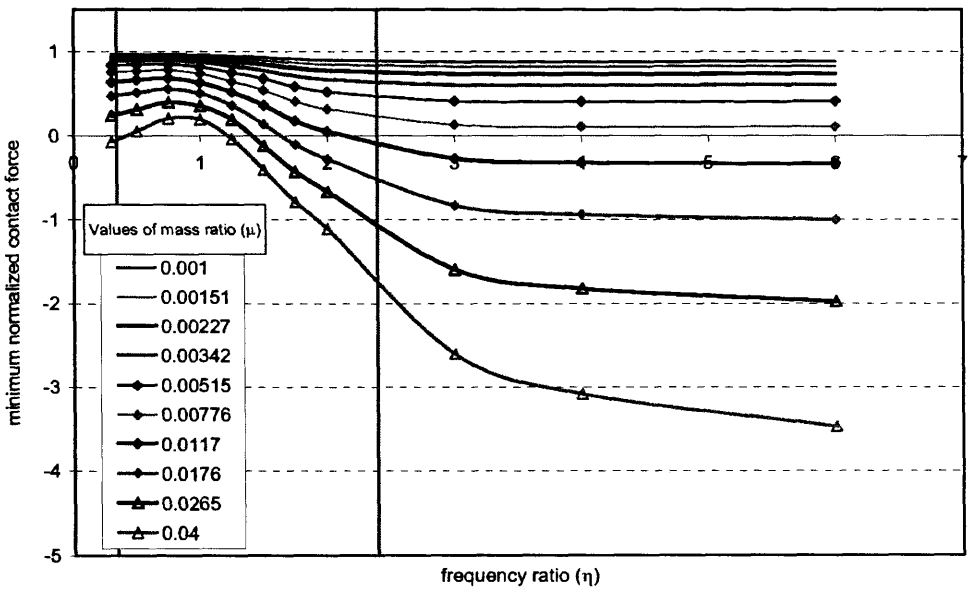

Figure 6. Minimum normalized contact force in first resonance situation. L/d = 0.75

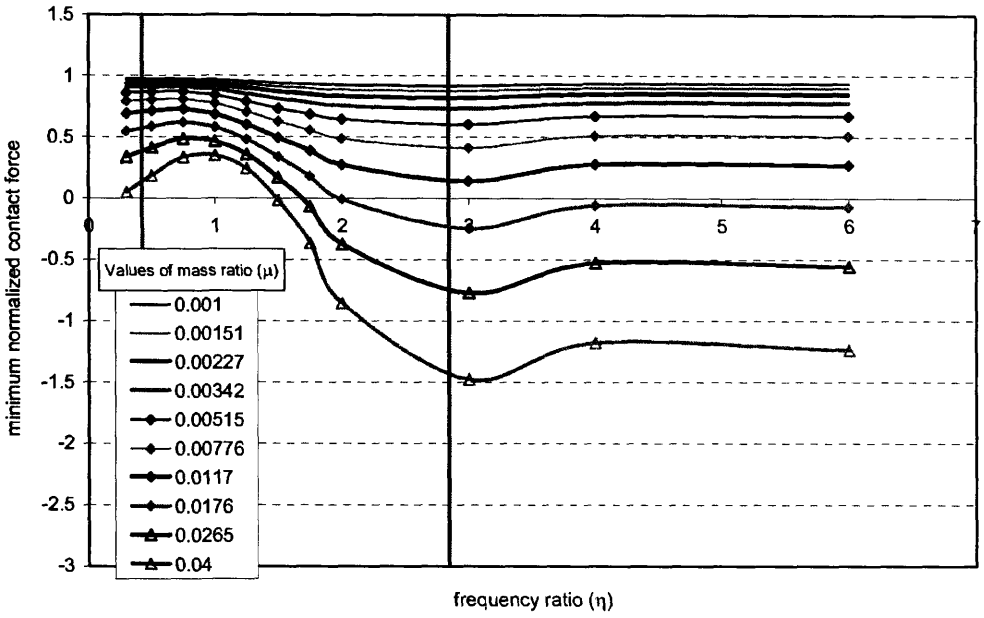

Figure 7. Minimum normalized contact force in first resonance situation. $L/d = 1$

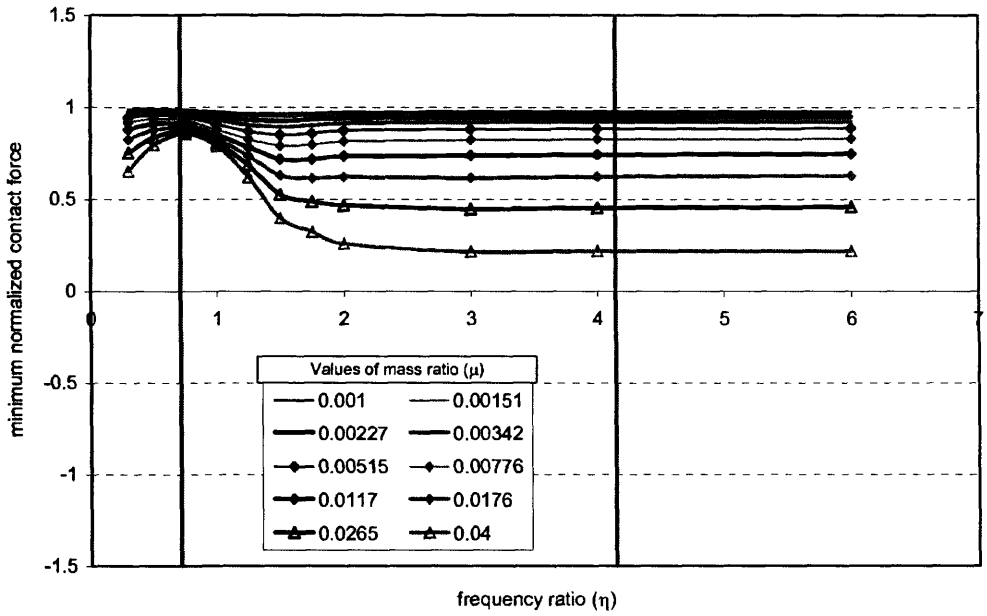

Figure 8. Minimum normalized contact force in first resonance situation. $L/d = 2$

In order to investigate whether a loss of contact could take place in real structures, a set of twenty seven reference bridges of spans ranging from 10 to 50 meters has been defined. Three different types of bridges have been considered: light composite bridges, medium–weight concrete box girder bridges and, finally, heavy concrete slab bridges. Their characteristics are shown in Table 2. The bridges have been designed for carrying one track, which implies that they have approximately half the mass of double–track bridges. As it is apparent from Figures 6, 7 and 8, this favours the likelihood of a loss of contact because light bridges imply high values of the mass ratio. Besides, the assumption of 1% structural damping is unfavourable for the shortest concrete bridges (where a higher value would be expected), but for the longer composite bridges it turns out to be favourable (see [**3**]). These two aspects ought to be taken into account before arriving to definitive conclusions.

	Composite Bridges		Box girder Bridges		Concrete Slab Bridges	
L (m)	m (kg/m)	n_0 (Hz)	m (kg/m)	n_0 (Hz)	m (kg/m)	n_0 (Hz)
10	9435	8.86	11046	15.60	17664	14.32
15	9561	6.75	11263	8.29	18373	6.95
20	9680	5.54	11784	6.52	16312	5.49
25	9805	4.79	12304	5.36	18337	4.49
30	9939	4.27	12825	4.55	20505	3.82
35	10093	4.02	13346	3.95	22455	3.31
40	10241	3.84	13866	3.49	25132	2.95
45	10395	3.68	14388	3.13	27180	2.64
50	10555	3.54	15096	2.83	29227	2.39

Table 2. Mechanical properties of twenty seven reference bridges

The bridges in Table 2 have been used for determining realistic combinations of parameters η and μ. To this end, the extreme values of n_t and m_t in modern trains have to be taken into account. Among the data available to the authors, the Spanish train Talgo features the higher frequency, n_t = 9.64 Hz and, simultaneously, the lower mass, m_t = 1406 kg. On the other hand, the English–French Eurostar presents the lower frequency, n_t = 5.84 Hz and the higher mass, m_t = 2900 kg (every two half–bogies of the SIM of this train are considered to vibrate almost simultaneously due to the little separation between them). Because very limited data are available regarding the mechanical characteristics of high–speed trains, a linear variation has been admitted between the values of n_t and m_t corresponding to the Talgo and the Eurostar; thus, an "intermediate" train having a semi–sprung mass of, say, 2000 kg, would have a frequency of the primary suspension equal to 8.13 Hz.

Combining the values in Table 2 with the characteristics of the Talgo and Eurostar three series of realistic combinations of η and μ can be obtained. Then, three curves can be fitted, each corresponding to a different type of bridge. The

curves are depicted in Figure 9, where the diamonds and triangles represent the combinations leading to a loss of contact for $L/d = 0.75$ and $L/d = 1$ respectively. As can be seen from that figures, the realistic pairs of frequency and mass ratios are quite distant from the dangerous values.

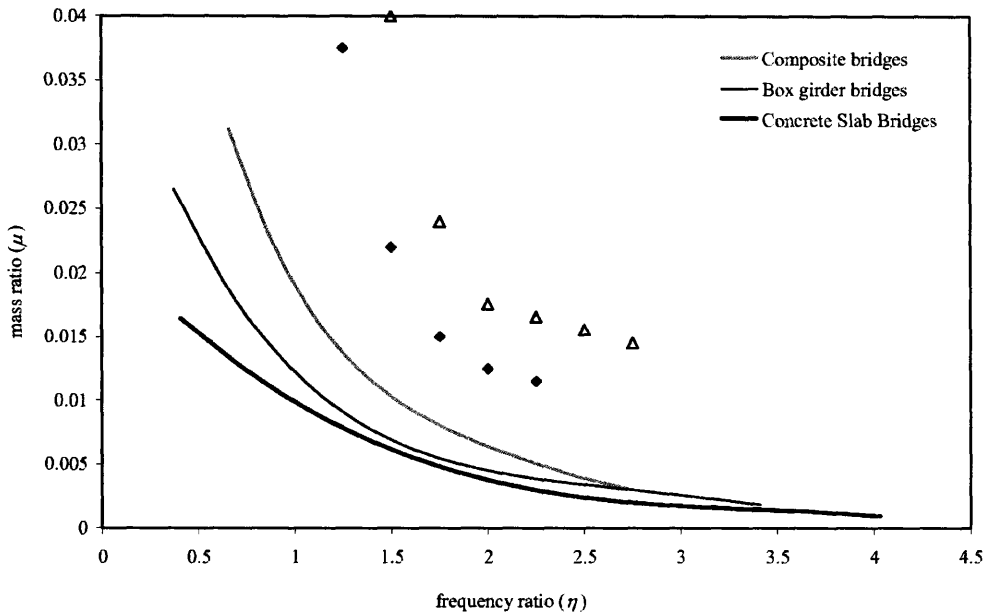

Figure 9. Realistic combinations of η and μ. Comparison with values leading to a loss of contact for $L/d = 0.75$ (♦) and $L/d = 1$ (Δ)

One last comment should be made regarding the analysis of the composite bridges. As mentioned before, a 1% structural damping is too favourable for such kind of bridges if the span is longer than approximately 15 m (see [3]). If the parametric study was carried out again with a lower value of ζ, the diamonds and triangles that represent the loss of contact in Figure 9 would lie closer to the curve corresponding to the composite bridges. This implies that light metal bridges with a low damping could be affected by such dangerous situations in case of resonance.

Nevertheless, it is very unlikely that a light, single-track, simply supported composite or metal bridge be designed for a high-speed line nowadays. The first reason is that double-track bridges are much more usual than the ones carrying one track and, besides, such kind of structures probably wouldn't be adequate to satisfy the acceleration SLI ($a_{max} < 3.5$ m/s^2). Whether double-track bridges could suffer from resonances associated to torsional oscillations, and the effects of such kind of behaviour on the wheel–rail contact forces, is a question that requires further study.

4 Analysis of a Real Example

In this section the minimum values of the wheel–rail contact forces in a simply supported bridge subjected to the passage of the Eurostar train are investigated. The purpose of this analysis is to ascertain whether the results obtained from the theoretical train with 15 equidistant loads differ markedly from those obtained when real high–speed trains are considered.

Following the approach of the dimensionless formulation of the equations of motion, twenty five bridges of span L = 17.5 m have been analysed. Five different natural frequencies have been considered, equally spaced between the range of values that can be considered habitual for this value of the span: $n_0 \in$ [4.5Hz, 11Hz]. This range corresponds to the limit of validity of the design method based on the Impact Factor as prescribed by Eurocode [**4**]. Considering that n_t = 5.84 for the Eurostar, the following five values of the frequency ratio are obtained: 1.30, 0.95, 0.75, 0.62, 0.53. For each value of the frequency ratio, five different values of the linear mass of the bridge have been analysed: 8000, 11000, 14000, 17000 and 20000 kg/m. Since the semi–sprung mass of the Eurostar is equal to 2900 kg, the resulting mass ratios are: 0.021, 0.015, 0.012, 0.010, 0.008.

The speed of the train has been selected in each case so as to produce the first resonance condition $V = n_0 \cdot d$ (d is close to 19 meters for the Eurostar). In this case the resonant speed is lower than 420 km/h only when η = 1.3 and 0.95, but the other cases have been also analysed for allowing the comparison with the results obtained with the theoretical train. In addition, an appropriate range of values of speed has been considered around $n_0 \cdot d$ in order to detect the maximum response of the bridge. The two models described in Section 1, DIM and SIM, have been used. The interaction force selected as the object of the analysis is the one corresponding to the last wheel of a passenger car (wheel number 44).

Figure 10 shows the results for the 25 bridges. As can be seen, the tendencies of the curves are similar to the ones in Figure 7. Again, the higher the mass of the bridge (the lower the mass ratio), the lower the variation of the contact force from its static value. In this regard, the theoretical train predicts correctly the real behaviour.

Finally, Figure 11 shows the comparison of the results obtained with the Eurostar and the theoretical train. It can be seen that the results of the DIM and SIM are quite similar, being ones more pessimistic than the others and vice versa depending on the particular value of the frequency ratio. A number of examples analysed during the development of the investigation showed that the car–bodies and secondary suspension helped reducing the oscillations of the contact forces (*i.e.* showed that the SIM was a pessimistic model), but this particular example demonstrates that this is not necessarily so. Also, it can be seen that in this example the theoretical train gives a rough but useful approximation to the behaviour of the contact forces of the Eurostar. This can not be expected if the number of repeated groups of loads of the

real train is not close to 15, or in a very short bridge where the movement of the two wheelsets of each bogie is significantly different. Also, it is remarkable that the minimum values of the real contact forces are sometimes smaller than the minimum values of the corresponding theoretical ones.

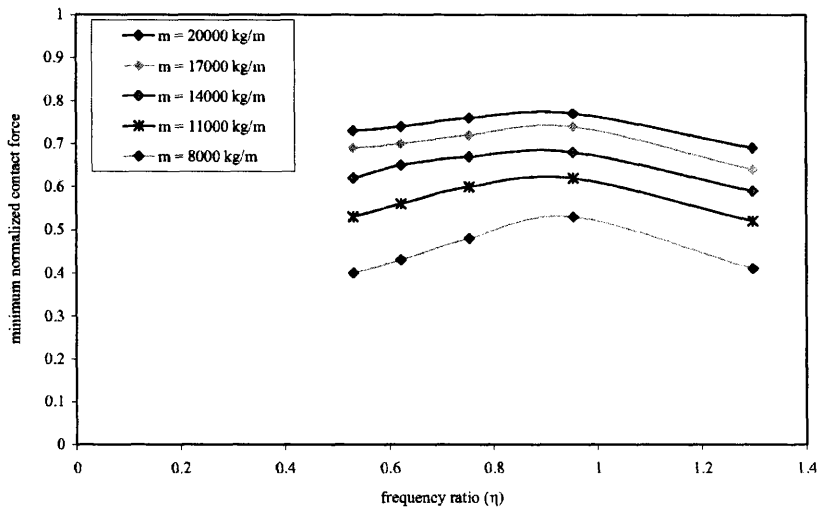

Figure 10. Minimum normalized contact force for 25 bridges of L = 17.5 m under the passage of the Eurostar train (DIM) at resonance

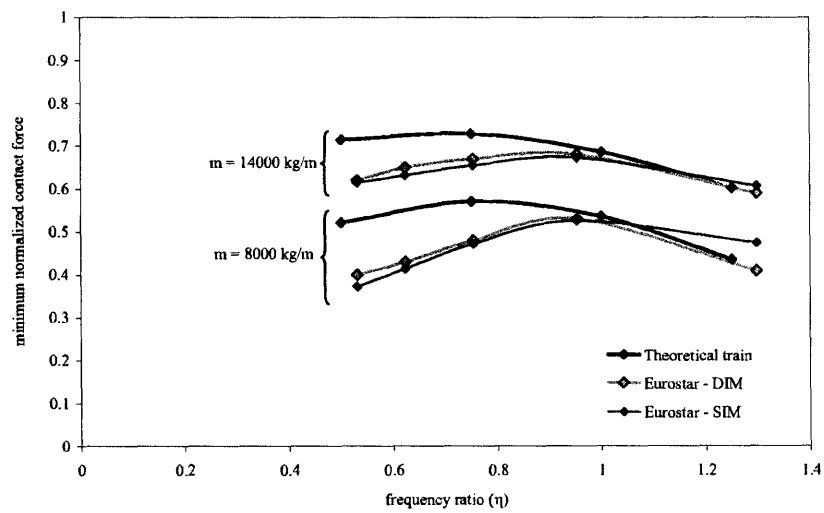

Figure 11. Minimum normalized contact force for bridges of L = 17.5 m, with mass per unit length 8000 and 14000 kg/m, under the passage of the Eurostar train (DIM and SIM) at resonance. Comparison with the theoretical train of 15 axles.

5 Conclusions

The following conclusions can be drawn from the investigations reported herein. It should be emphasised that during the completion of these studies the effects of rail and wheel irregularities have not been taken into account.

(1) In resonance situation the mechanical models capable of taking into account the train–bridge interaction effects are less pessimistic that the Travelling Loads Models. Therefore, if the characteristics of the high-speed vehicles and the bridges are reliably known a priori, the Simplified or the Detailed Interaction Models can be used for obtaining a more optimized design.

(2) The wheel–rail contact forces undergo oscillations during the passage of the axles over the bridge. During resonance, these oscillations are more severe for the rear wheels than for the front ones.

(3) If L denotes the span of a simply supported bridge, and d the characteristic distance between consecutive groups of loads, the lower the value of L/d, the greater the oscillations of the contact forces at resonance. For $L/d = 2$ or greater, no likelihood of loss of wheel–rail contact has been detected.

(4) The ratio between the frequency of the primary suspension of the vehicle and the fundamental frequency of the bridge is denoted by η (frequency ratio), and the ratio of the semi–sprung mass of the vehicle (mass of the bogie) and the total mass of the bridge is denoted by μ (mass ratio). For any given frequency ratio, the greater the mass ratio, the greater the oscillations of the contact forces at resonance.

(5) The oscillations of the contact forces at resonance, and therefore the likelihood of loss of wheel–rail contact, present a minimum for η approximately between 0.5 and 1. For lower or higher values of the frequency ratio the oscillations of the contact forces increase.

(6) Neglecting the possible effects of torsional vibrations, the metal or composite bridges with a low linear mass have been found to be the ones where the contact forces may suffer the most severe oscillations. If single-track, simply supported, composite or metal bridges were used in high-speed lines, and damping ratios below 1% were expected, the minimum contact forces at resonance could drop to dangerous values. Nevertheless, this kind of structures is very unusual in modern high-speed railway lines.

References

[1] Y.K. Cheung, F.T.K. Au, D.Y. Zheng, Y.S. Cheng, "*Vibration of multi-span non-uniform bridges under moving vehicles and trains by using modified beam vibration functions*", Journal of Sound and Vibration, 228(3), 611-628, 1999.

[2] ERRI D214 Committe, "*Ponts-rails pour vitesses > 200 km/h. Rapport 4. Interaction train-pont*", Technical Report, European Rail Research Institute, Utretch, The Netherlands, 1998.

[3] ERRI D214 Committe, "*Ponts-rails pour vitesses > 200 km/h. Rapport final*", Technical Report, European Rail Research Institute, Utretch, The Netherlands, 1999.

[4] European Committee for Standardization (CEN), "*Eurocode 1: Actions on structures. Part 2: General actions—Traffic loads on bridges. Final Draft prEN 1991-2*", Brussels, 2002.

[5] S.H. Ju, H.T. Lin, "*Resonance characteristics of high-speed trains passing simply supported bridges*", Journal of Sound and Vibration, 267, 1127-1141, 2003.

[6] M. Klasztorny, J. Langer. "*Dynamic response of single-span beam bridges to a series of moving loads*". Earthquake Engineering and Structural Dynamics, 19, 1107-1124, 1990.

[7] J.W. Kwark, E.S. Choi, Y.J. Kim, B.S. Kim, S.I. Kim, "*Dynamic behavior of two-span continuous concrete bridges under moving high-speed train*", Computers & Structures, 82, 463-474, 2004

[8] P. Museros, G. Vivero and E. Alarcón, "*Moving loads on railway bridges: the Spanish Code Approach*", Proceedings of the 4th European Conference of Structural Dynamics (Eurodyn '99), 675-680, A.A. Balkema, 1999.

[9] P. Museros and E. Alarcón. "*An investigation on the importance of train-bridge interaction at resonance*", Proceedings of the 6th International Conference on Computational Structures Technology (CST–2002), 335-336, Civil-Comp Press, Stirling (Scotland), 2002.

[10] P. Museros, A. Poy, M. Romero and E. Alarcón. "*Advances in the analysis of short span railway bridges for high speed lines*", Computers & Structures, 80 (27-30), 2121-2132, 2002.

[11] P. Museros and E. Alarcón. "*Influence of the second bending mode on the response of high–speed bridges*", Proceedings of the 9th International Conference on Civil and Structural Engineering Computing (CC–2003), 197-198, Civil-Comp Press, Stirling (Scotland), 2003.

[12] M.K. Song, H.C. Noh, C.K. Choi, "*A new three-dimensional finite element analysis model of high-speed train–bridge interactions*". Engineering Stuctures, 25, 1611-1626, 2003.

[13] Y.B. Yang and J.D. Yau, "*Vehicle-bridge interaction element for dynamic analysis*", Journal of Structural Engineering, 123(11), 1512-1518, 1997.

[14] Y.B. Yang, J.D. Yau y L.C. Hsu, "*Vibration of simple beams due to trains moving at high speeds*", Engineering Structures, 19(11), 936-944, 1997.